Three- or Two-Stage Stochastic Market-Clearing Algorithm?

Farzaneh Abbaspourtorbati, *Student Member, IEEE*, Antonio J. Conejo, *Fellow, IEEE*, Jianhui Wang, *Senior Member, IEEE*, and Rachid Cherkaoui, *Senior Member, IEEE*

***Abstract*—As the power industry considers moving from a deterministic paradigm to a stochastic one to clear the day-ahead market in systems with significant stochastic production, the following question arises: how should a stochastic clearing algorithm be formulated? Our analyses indicate that a three-stage stochastic approach is clearly superior to a two-stage one. To show this, we propose a model that includes three stages: the first one represents the day-ahead market, the second stage, the intraday market, and the third one, the real-time operation. The objective is to clear the day-ahead market, but with a prognosis of the future: the intraday market and the real-time operation. To assess the impact of the intraday market on the day-ahead outcomes, we compare the results obtained from the proposed model with those of a simpler but more common two-stage model, which represents the day-ahead market and the real-time operation.**

***Index Terms*—Market-clearing model, nonconvexities, stochastic programming.**

NOTATION

The notation is provided below.

Superscripts, Indices and Sets

t	Index of time periods running from 1 to N_{T}
n	Index of nodes running from 1 to N_{N}.
i	Index of generating units running from 1 to N_{G}.
j	Index of loads running from 1 to N_{L}.
ω	Index of path for wind power scenarios running from 1 to N_{Ω}.
q	Index of wind units running from 1 to N_{Q}.
Λ_n	Set of nodes directly connected to node n.
M_n^{G}	Set of generating units located at node n.
M_n^{L}	Set of loads located at node n.
M_n^{Q}	Set of wind units located at node n.
s_1	Superscript denoting the day-ahead market (first stage).
s_2	Superscript denoting the intra-day market (second stage).
s_3	Superscript denoting the real-time operation (third stage).

Constants

α^{WUs_1}	Constant determining the upper limit of wind power output at the day-ahead market.
α^{WDs_1}	Constant determining the lower limit of wind power output at the day-ahead market.
α^{WUs_2}	Constant determining the upper limit of wind power output at the intra-day market.
α^{WDs_2}	Constant determining the lower limit of wind power output at the intra-day market.
$\alpha_{\Delta W}$	Constant determining the upper limit of wind adjustments at the intra-day market.
$\alpha_{\Delta P}$	Constant determining the upper limit of conventional unit adjustments at the intra-day market.
π_ω	Probability of wind power scenario path ω.
L_{jt}	Power consumption by load j in period t [MW].
$P_i^{\max}$	Capacity of unit i [MW].
$P_i^{\min}$	Minimum power output of unit i [MW].
$f_{\mathrm{nr}}^{\max}$	Transmission capacity of line (nr) [MW].
C_q	Marginal production cost of wind unit q [$/MWh].
C_i	Marginal production cost of conventional unit i [$/MWh].
K_i^{SU}	Start-up cost of conventional unit i [$/MWh].
$R_i^{\mathrm{D,max}}$	Maximum down-reserve for unit i [MW].
$R_i^{\mathrm{U,max}}$	Maximum up-reserve for unit i [MW].
V_j^{LOL}	Value of lost load for load j [$/MWh].
$W_q^{\max}$	Maximum power production of wind unit q [MW].
$W_{\mathrm{qt}}^{\mathrm{s}_1}$	Best forecast of wind power generation for unit q at stage s_1 and period t [MW].
$W_{\mathrm{qt}\omega}^{\mathrm{s}_2}$	Best forecast of wind power generation for unit q in scenario ω at stage s_2 and period t [MW].
$W_{\mathrm{qt}\omega}^{\mathrm{s}_3}$	Realization of wind power generation for unit q in scenario ω at stage s_3 and period t [MW].
B_{nr}	Susceptance of line (nr) [per unit].
RU_i	Ramp-up limit of unit i [MW/h].
RD_i	Ramp-down limit of unit i [MW/h].

First-stage Variables (Day-ahead Market)

$C_{\mathrm{it}}^{\mathrm{SU}}$	Start-up cost of conventional unit i in period t [$].
P_{it}	Power scheduled for unit i at the day-ahead market in period t [MW].

Manuscript received April 18, 2016; revised August 23, 2016 and October 12, 2016; accepted October 21, 2016. Date of publication October 25, 2016; date of current version June 16, 2017. The work of F. Abbaspourtorbati was supported by Swissgrid. The work of A. J. Conejo was supported in part by Argonne National Laboratory and in part by NSF under Grant 60050502. Paper no. TPWRS-00604-2016.

F. Abbaspourtorbati is with Swissgrid, Laufenburg 5080, Switzerland, and also with EPFL, Lausanne 1015, Switzerland (e-mail: farzaneh.abbaspourtorbati@epfl.ch).

A. J. Conejo is with the Integrated System Engineering and the Electrical & Computer Engineering Departments, The Ohio State University, Columbus, OH 43210 USA (e-mail: conejonavarro.1@osu.edu).

J. Wang is with Argonne National Laboratory, Argonne, IL 60439 USA (e-mail: jianhui.wang@anl.gov).

R. Cherkaoui is with EPFL, Lausanne 5080, Switzerland (e-mail: Rachid.Cherkaoui@epfl.ch).

Color versions of one or more of the figures in this paper are available online at http://ieeexplore.ieee.org.

Digital Object Identifier 10.1109/TPWRS.2016.2621069

θ_{nt} Angle of node n at the day-ahead market in period t [rad].
W_{qt} Power scheduled for wind unit q at the day-ahead market in period t [MW].
u_{it} Binary variables that is equal to 1 if unit i is scheduled to be committed in period t.

Second-stage Variables (Intra-day Market)

$\Delta P^{\mathrm{U}}_{\mathrm{it}\omega}$ Upward power adjustment for unit i in scenario ω and period t at the intra-day market [MW].
$\Delta P^{\mathrm{D}}_{\mathrm{it}\omega}$ Downward power adjustment for unit i in scenario ω and period t at the intra-day market [MW].
$\Delta W^{\mathrm{U}}_{\mathrm{qt}\omega}$ Upward power adjustment for wind unit q in scenario ω and period t at the intra-day market [MW].
$\Delta W^{\mathrm{D}}_{\mathrm{qt}\omega}$ Downward power adjustment for wind unit q in scenario ω and period t at the intra-day market [MW].
$\theta^{\mathrm{s_2}}_{\mathrm{nt}\omega}$ Angle of node n in scenario ω and period t at the intra-day market [rad].

Third-stage Variables (Real-time Operation)

$r^{\mathrm{U}}_{\mathrm{it}\omega}$ Deployed up reserve by unit i in scenario ω and period t at the operation stage [MW].
$r^{\mathrm{D}}_{\mathrm{it}\omega}$ Deployed down reserve by unit i in scenario ω and period t at the operation stage [MW].
$\theta^{\mathrm{s_3}}_{\mathrm{nt}\omega}$ Angle of node n in scenario ω and period t at the operation stage [rad].
$w^{\mathrm{spill}}_{\mathrm{qt}\omega}$ Wind power spillage of unit q in scenario ω and period t at the operation stage [MW].
$L^{\mathrm{shed}}_{\mathrm{jt}\omega}$ Involuntarily load shedding of load j in scenario ω and period t at the operation stage [MW].

I. Introduction

As THE power industry considers moving from a deterministic day-ahead market to a stochastic one in systems with significant stochastic production, a key question is: how such stochastic clearing algorithms should actually be. We show in this paper that a three-stage mode is clearly superior to a two-stage one. However, many references focus on two-stage stochastic models that include a first stage representing the day-ahead market and a second stage describing the system operation [1]–[7]. Similarly, adaptive robust optimization [8] minimizes the total cost in the worst-case realization of the uncertainty, and the recourse actions are taken after the uncertainties are realized in real-time operation [9]–[12]. With the purpose of obtaining a solution that balances the operating cost and robustness, [13] introduce a hybrid unit-commitment formulation that merges stochastic unit commitment and interval unit commitment [14]. Also, [15] proposes an approach that unifies scenario-based stochastic unit commitment and robust unit commitment.

It is important to note that an increasing number of electricity markets with large renewable production include intra-day markets, of which explicit models are missed in the technical literature. Such intra-day markets give stochastic units the opportunity of offering closer to power delivery and thus with reduced uncertainty. The current market structure, hence, includes a day-ahead market settling 24 hourly-based schedules with a gate closure in day d-1, an intra-day market settling 24 hourly-based adjustments with a gate-closure usually several hours ahead of power delivery, a real-time market for final balancing transactions with gate-closures several minutes ahead of power delivery, and real-time operation. Thus, corresponding to each time period t in day d there are four points in time when the operator makes a decision: the scheduling decision in the day-ahead market with a gate closure in day d-1, the adjustment decision in the intra-day market with a gate closure several hours ahead of power delivery (in day d-1), and the real-time market gate closures of several minutes ahead of power delivery (in day d), and the deployed reserve decision in real-time. For the sake of simplicity, we merge the real-time market and the real-time operation.

In the above context, this paper proposes a three-stage stochastic model to clear the day-ahead market, where uncertainty stems from stochastic wind generation. The first stage represents the day-ahead market, the second stage the intra-day market, and the third stage the real-time operation. Therefore, the day-ahead schedules are decided with a detailed prognosis of the future, which includes the intra-day market and real-time operation. Non-convexities due to start-up costs of generators and their minimum power output are modeled using Mixed-Integer Linear Programming (MILP). Clearing prices are obtained using a relaxed version of the MILP problem.

It should be emphasised that the proposed model is intended to directly replace simplistic deterministic day-ahead market-clearing models. The outcome of both the proposed model and a deterministic model are day-ahead clearing quantities and prices, but the proposed model derives such quantities with an informed prognosis of the future. This results in a day-ahead outcome "adapted" to the uncertainty involved. On the contrary, a deterministic model generally results in either under-commitment, which is risky, or over-commitment, which is expensive.

Since references comparing deterministic vs. two-stage stochastic approaches abound in the technical literature [4], [16], [17], we concentrate on comparing a three-stage approach with a two-stage one that does not incorporate a prognosis of the intra-day market. In other words, while a two-stage model represents only the operation stage, a three-stage model represents both the intra-day market and the operation stage. Therefore, we investigate the effects of representing the intra-day market on day-ahead results.

The novel contribution of this paper is twofold:

1) To introduce a three-stage stochastic programming model to clear the day-ahead market with a prognosis of the intra-day market and the real-time operation.
2) To show that replacing a deterministic model with a three-stage stochastic model, not a two-stage one, results in better outcomes without significantly increasing the required computational burden.

The rest of the paper is organized as follows. Section II provides the mathematical formulation of the proposed three-stage model. An illustrative example is provided in Section III. Section IV reports and discusses results from a realistic case study. Some conclusions are provided in Section V.

II. Market Model

Market-clearing model (1) below co-optimizes energy and reserve. We use a DC representation of the transmission net-

work, since the simultaneous consideration of on/off decisions, stochasticity and an AC power flow model leads necessarily to intractability. We also consider the following simplifying assumptions, which can be removed not altering the nature of the model:

1) Uncertainty pertains only to wind generation.
2) Generation cost functions are assumed to be linear.
3) The cost of deploying reserve is the cost of energy production.
4) Loads are assumed to be inelastic.

The MILP market-clearing model is:

$$\underset{\Xi_p}{\text{Minimize}}$$

$$\sum_{t=1}^{N_T}\left[\sum_{i=1}^{N_G} C_{\mathrm{it}}^{\mathrm{SU}} + \sum_{\omega=1}^{N_\Omega}\pi_\omega\left[\sum_{i=1}^{N_G} C_i(P_{\mathrm{it}} + \Delta P_{\mathrm{it}\omega}^{\mathrm{U}} - \Delta P_{\mathrm{it}\omega}^{\mathrm{D}} + r_{\mathrm{it}\omega}^{\mathrm{U}} - r_{\mathrm{it}\omega}^{\mathrm{D}}) + \sum_{q=1}^{N_Q} C_q(W_{\mathrm{qt}\omega}^{\mathrm{s}_3} - w_{\mathrm{qt}\omega}^{\mathrm{spill}}) + \sum_{j=1}^{N_L} V_{\mathrm{jt}}^{\mathrm{LOL}} L_{\mathrm{jt}\omega}^{\mathrm{shed}}\right]\right] \quad (1a)$$

subject to

first-stage constraints:

$$\sum_{i\in M_n^{\mathrm{G}}} P_{\mathrm{it}} + \sum_{q\in M_n^{\mathrm{Q}}} W_{\mathrm{qt}} - \sum_{j\in M_n^{\mathrm{L}}} L_{\mathrm{jt}} - \sum_{r\in\Lambda_n} B_{\mathrm{nr}}(\theta_{\mathrm{nt}} - \theta_{rt}) = 0, \forall n, \forall t \quad (1b)$$

$$u_{\mathrm{it}} P_i^{\min} \le P_{\mathrm{it}} \le u_{\mathrm{it}} P_i^{\max}, \forall i, \forall t \quad (1c)$$

$$\alpha^{\mathrm{WDs}_1} W_{\mathrm{qt}}^{\mathrm{s}_1} \le W_{\mathrm{qt}} \le \alpha^{\mathrm{WUs}_1} W_{\mathrm{qt}}^{\mathrm{s}_1}, \forall q, \forall t \quad (1d)$$

$$K_i^{\mathrm{SU}}(u_{\mathrm{it}} - u_{i,t-1}) \le C_{\mathrm{it}}^{\mathrm{SU}}, \forall i, \forall t \quad (1e)$$

$$u_{\mathrm{it}} \in \{0,1\}, \forall i, \forall t \quad (1f)$$

$$RD_i \le P_{\mathrm{it}} - P_{i,t-1} \le RU_i, \forall i, \forall \omega, \forall t \quad (1g)$$

$$\theta_{1t} = 0 \quad (1h)$$

second-stage constraints:

$$\sum_{i\in M_n^{\mathrm{G}}} \Delta P_{\mathrm{it}\omega}^{\mathrm{U}} - \Delta P_{\mathrm{it}\omega}^{\mathrm{D}} + \sum_{q\in M_n^{\mathrm{Q}}} W_{\mathrm{qt}\omega}^{\mathrm{s}_2} - W_{\mathrm{qt}} - \Delta W_{\mathrm{qt}\omega}^{\mathrm{U}} + \Delta W_{\mathrm{qt}\omega}^{\mathrm{D}} - \sum_{r\in\Lambda_n} B_{\mathrm{nr}}(\theta_{\mathrm{nt}\omega}^{\mathrm{s}_2} - \theta_{rt\omega}^{\mathrm{s}_2} - \theta_{\mathrm{nt}} + \theta_{rt}) = 0, \forall n, \forall \omega, \forall t \quad (1i)$$

$$u_i P_i^{\min} \le P_{\mathrm{it}} + \Delta P_{\mathrm{it}\omega}^{\mathrm{U}} - \Delta P_{\mathrm{it}\omega}^{\mathrm{D}} \le u_{\mathrm{it}} P_i^{\max}, \forall i, \forall \omega, \forall t \quad (1j)$$

$$\alpha^{\mathrm{WDs}_2} W_{\mathrm{qt}\omega}^{\mathrm{s}_2} \le W_{\mathrm{qt}} + \Delta W_{\mathrm{qt}\omega}^{\mathrm{U}} - \Delta W_{\mathrm{qt}\omega}^{\mathrm{D}} \le \alpha^{\mathrm{WUs}_2} W_{\mathrm{qt}\omega}^{\mathrm{s}_2}, \forall q, \forall \omega, \forall t \quad (1k)$$

$$\Delta P_{\mathrm{it}\omega}^{\mathrm{U}} \le \alpha_{\Delta P} P_i^{\max}; \Delta P_{\mathrm{it}\omega}^{\mathrm{D}} \le \alpha_{\Delta P} P_i^{\max}, \forall i, \forall \omega, \forall t \quad (1l)$$

$$\Delta W_{\mathrm{qt}\omega}^{\mathrm{U}} \le \alpha_{\Delta W} W_q^{\max}; \Delta W_{\mathrm{qt}\omega}^{\mathrm{D}} \le \alpha_{\Delta W} W_q^{\max}, \forall q, \forall \omega, \forall t \quad (1m)$$

$$RD_i \le P_{\mathrm{it}} + \Delta P_{\mathrm{it}\omega}^{\mathrm{U}} - \Delta P_{\mathrm{it}\omega}^{\mathrm{D}} - P_{i,t-1} - \Delta P_{i,t-1,\omega}^{\mathrm{U}} + \Delta P_{i,t-1,\omega}^{\mathrm{D}} \le RU_i, \forall i, \forall \omega, \forall t \quad (1n)$$

$$\theta_{1t\omega}^{\mathrm{s}_2} = 0 : \sigma_{1t\omega}, \forall \omega, \forall t \quad (1o)$$

third-stage constraints:

$$\sum_{q\in M_n^{\mathrm{Q}}} (W_{\mathrm{qt}\omega}^{\mathrm{s}_3} - W_{\mathrm{qt}} - \Delta W_{\mathrm{qt}\omega}^{\mathrm{U}} + \Delta W_{\mathrm{qt}\omega}^{\mathrm{D}} - w_{\mathrm{qt}\omega}^{\mathrm{spill}}) + \sum_{i\in M_n^{\mathrm{G}}} (r_{\mathrm{it}\omega}^{\mathrm{U}} - r_{\mathrm{it}\omega}^{\mathrm{D}}) - \sum_{r\in\Lambda_n} B_{\mathrm{nr}}(\theta_{\mathrm{nt}\omega}^{\mathrm{s}_3} - \theta_{rt\omega}^{\mathrm{s}_3} - \theta_{\mathrm{nt}\omega}^{\mathrm{s}_2} + \theta_{rt\omega}^{\mathrm{s}_2}) + \sum_{j\in M_n^{\mathrm{L}}} L_{\mathrm{jt}\omega}^{\mathrm{shed}} = -0, \forall n, \forall \omega, \forall t \quad (1p)$$

$$u_{\mathrm{it}} P_i^{\min} \le P_{\mathrm{it}} + \Delta P_{\mathrm{it}\omega}^{\mathrm{U}} - \Delta P_{\mathrm{it}\omega}^{\mathrm{D}} + r_{\mathrm{it}\omega}^{\mathrm{U}} - r_{\mathrm{it}\omega}^{\mathrm{D}} \le u_{\mathrm{it}} P_i^{\max}, \forall i, \forall \omega, \forall t \quad (1q)$$

$$r_{\mathrm{it}\omega}^{\mathrm{U}} \le R_i^{\mathrm{U,max}}, \forall i, \forall \omega, \forall t \quad (1r)$$

$$r_{\mathrm{it}\omega}^{\mathrm{D}} \le R_i^{\mathrm{D,max}}, \forall i, \forall \omega, \forall t \quad (1s)$$

$$L_{\mathrm{jt}\omega}^{\mathrm{shed}} \le L_{\mathrm{jt}}, \forall j, \forall \omega, \forall t \quad (1t)$$

$$w_{\mathrm{qt}\omega}^{\mathrm{spill}} \le W_{\mathrm{qt}\omega}^{\mathrm{s}_3}, \forall q, \forall \omega, \forall t \quad (1u)$$

$$-f_{\mathrm{nr}}^{\max} \le B_{\mathrm{nr}}(\theta_{\mathrm{nt}\omega}^{\mathrm{s}_3} - \theta_{rt\omega}^{\mathrm{s}_3}) \le f_{\mathrm{nr}}^{\max}, \forall n, \forall r \in \Lambda_n, \forall \omega, \forall t \quad (1v)$$

$$RD_i \le P_{\mathrm{it}} + \Delta P_{\mathrm{it}\omega}^{\mathrm{U}} - \Delta P_{\mathrm{it}\omega}^{\mathrm{D}} + r_{\mathrm{it}\omega}^{\mathrm{U}} - r_{\mathrm{it}\omega}^{\mathrm{D}} - P_{i,t-1} - \Delta P_{i,t-1,\omega}^{\mathrm{U}} + \Delta P_{i,t-1,\omega}^{\mathrm{D}} - r_{i,t-1,\omega}^{\mathrm{U}} + r_{i,t-1,\omega}^{\mathrm{D}} \le RU_i, \forall i, \forall \omega, \forall t \quad (1w)$$

$$\theta_{1t\omega}^{s_3} = 0, \forall \omega, \forall t \quad (1x)$$

non-anticipativity constraints:

$$\Delta P_{\mathrm{it}\omega}^{\mathrm{U}} = \Delta P_{it\hat{\omega}}^{\mathrm{U}}, \Delta P_{\mathrm{it}\omega}^{\mathrm{D}} = \Delta P_{it\hat{\omega}}^{\mathrm{D}}, \forall i, \forall \omega, \hat{\omega} | \omega = \hat{\omega}, \forall t$$

$$\Delta W_{\mathrm{qt}\omega}^{\mathrm{U}} = \Delta W_{\mathrm{qt}\hat{\omega}}^{\mathrm{U}}, \Delta W_{q\omega}^{\mathrm{D}} = \Delta W_{q\hat{\omega}}^{\mathrm{D}}, \forall q, \forall \omega, \hat{\omega} | \omega = \hat{\omega}, \forall t$$

$$\theta_{\mathrm{nt}\omega}^{s_2} = \theta_{nt\hat{\omega}}^{s_2}, \forall n, \forall \omega, \hat{\omega} | \omega = \hat{\omega}, \forall t \quad (1y)$$

variable declaration:

$$0 \le P_{\mathrm{it}}, C_{\mathrm{it}}^{\mathrm{SU}}, \forall i, \forall t; \quad 0 \le W_{\mathrm{qt}}, \forall q, \forall t$$

$$0 \le \Delta P_{\mathrm{it}\omega}^{\mathrm{U}}, \Delta P_{\mathrm{it}\omega}^{\mathrm{D}}, r_{\mathrm{it}\omega}^{\mathrm{U}}, r_{\mathrm{it}\omega}^{\mathrm{D}}, \forall i, \forall \omega, \forall t$$

$$0 \le \Delta W_{\mathrm{qt}\omega}^{\mathrm{U}}, \Delta W_{\mathrm{qt}\omega}^{\mathrm{D}}, w_{\mathrm{qt}\omega}^{\mathrm{spill}}, \forall q, \forall \omega, \forall t$$

$$0 \le L_{\mathrm{jt}\omega}^{\mathrm{shed}}, \forall j, \forall \omega, \forall t \quad (1z)$$

where $\Xi_p = \{C_{\mathrm{it}}^{\mathrm{SU}}, u_{\mathrm{it}}, P_{\mathrm{it}}, W_{\mathrm{qt}}, \theta_{\mathrm{nt}}, \Delta P_{\mathrm{it}\omega}^{\mathrm{U}}, \Delta P_{\mathrm{it}\omega}^{\mathrm{D}}, \Delta W_{\mathrm{qt}\omega}^{\mathrm{U}}, \Delta W_{\mathrm{qt}\omega}^{\mathrm{D}}, r_{\mathrm{it}\omega}^{\mathrm{U}}, r_{\mathrm{it}\omega}^{\mathrm{D}}, w_{\mathrm{qt}\omega}^{\mathrm{spill}}, \theta_{\mathrm{nt}\omega}^{s_2}, \theta_{\mathrm{nt}\omega}^{s_3}, L_{\mathrm{jt}\omega}^{\mathrm{shed}}\}$ is the set of variables.

The objective function (1a) is the expected operation costs. It includes start-up and energy costs of conventional units, the cost of wind units, and the cost of involuntary load shedding.

Constraint (1b) represents the power balance at the day-ahead market, where the units are scheduled. Constraints (1c) and (1d) enforce the limits of conventional generation and wind production, respectively, at the day-ahead market. Constraint (1e) stands for the start-up costs that depends on the on/off status of each generating unit via binary variable u_{it} in (1f). Ramping constraints of conventional units are enforced by (1g) at the

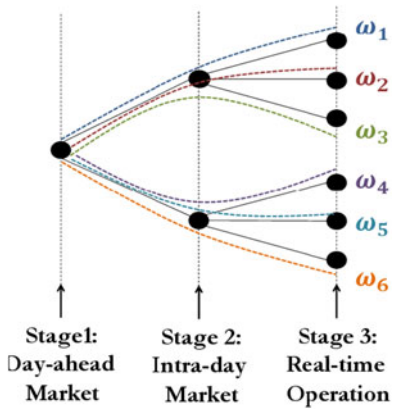

Fig. 1. Scenario tree and scenario paths for a three-stage market-clearing model.

day-ahead market. Constraint (1h) states that node 1 is the reference node at the day-ahead market.

Constraint (1i) stands for the power balance at the intra-day market, where scheduled productions are adjusted. The production limits of conventional and wind units when adjusting first-stage schedules shall be respected in the intra-day market as stated in (1j) and (1k), respectively. In the intra-day market, the up and down adjustments of conventional units are assumed to be limited to $\alpha_{\Delta P}\%$ of the maximum power outputs as enforced by (1l). Also, (1m) enforces that up and down adjustments of wind production are limited to $\alpha_{\Delta W}\%$ of the wind installed capacity at the intra-day stage. Ramping constraints of conventional units at the intra-day market are enforced by (1n). Constraint (1o) identifies the reference node at the intra-day stage.

At the operation stage, (1p) represents the power balance, where deployed reserves and curtailed loads compensate for wind deviations. The line flow limits are enforced by (1v). The reserve deployment shall respect the generation limits at the actual operation, which is stated in (1q). Constraints (1r) and (1s) represent maximum up and down reserves, respectively. The limits of load curtailments and wind spillage are enforced by (1t) and (1u), respectively. Constraint (1w) enforces ramping limits of conventional units at the operation stage.

The reference node at the operation stage is node 1 as stated by (1x). Equation (1y) represents non-anticipativity of up and down unit adjustments, up and down adjustments of wind production, and angles at the intra-day stage. Non-negativity of start-up costs, productions, deployed reserves, wind spillage, and load shedding are enforced by (1z).

Note that ω represents a scenario path; that is, a realization of the wind production at each stage. Fig. 1 depicts the scenario paths for the three-stage market model in (1) considering two scenarios at the second stage and three scenarios at the third stage. The non-anticipativity of the decisions at the second stage let $\theta^{\mathrm{s2}}_{n\omega_1} = \theta^{\mathrm{s2}}_{n\omega_2} = \theta^{\mathrm{s2}}_{n\omega_3}$ and $\theta^{\mathrm{s2}}_{n\omega_4} = \theta^{\mathrm{s2}}_{n\omega_5} = \theta^{\mathrm{s2}}_{n\omega_6}$, $\Delta P^{\mathrm{U}}_{i\omega_1} = \Delta P^{\mathrm{U}}_{i\omega_2} = \Delta P^{\mathrm{U}}_{i\omega_3}$ and $\Delta P^{\mathrm{U}}_{i\omega_4} = \Delta P^{\mathrm{U}}_{i\omega_5} = \Delta P^{\mathrm{U}}_{i\omega_6}$, $\Delta W^{\mathrm{U}}_{q\omega_1} = \Delta W^{\mathrm{U}}_{q\omega_2} = \Delta W^{\mathrm{U}}_{q\omega_3}$ and $\Delta W^{\mathrm{U}}_{q\omega_4} = \Delta W^{\mathrm{U}}_{q\omega_5} = \Delta W^{\mathrm{U}}_{q\omega_6}$, and similar equalities for downward schedule adjustments.

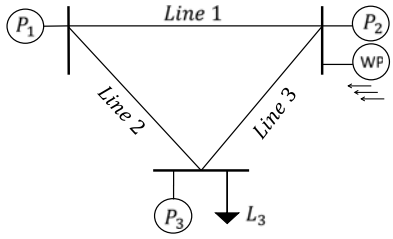

Fig. 2. Test system.

TABLE I
DATA OF GENERATING UNITS

unit i	K_i^{SU} (\$)	C_i (\$/MW)	$P_i^{\max}$ (MW)	$P_i^{\min}$ (MW)
1	10.01	3.03	102.00	10.00
2	10.20	4.01	101.00	10.00
3	50.06	5.09	100.00	10.00

TABLE II
WIND SCENARIOS [MW] OVER TIME PERIODS 1 AND 2

	period 1		period 2	
scenarios	ID stage	RT stage	ID stage	RT stage
(High, High)	60	91	89	99
(High, Medium)	60	71	89	85
(High, Low)	60	49	89	21
(Low, High)	35	67	46	91
(Low, Medium)	35	37	46	48
(Low, Low)	35	9	46	11

III. ILLUSTRATIVE EXAMPLE

To illustrate the advantages of the proposed market-clearing model, the three-node system depicted in Fig. 2 is considered. The planning horizon spans two time periods. Line reactances and capacities are all equal to 0.13 p.u. and 500 MW, respectively. The system includes three conventional units and one wind unit. The data of conventional units are provided in Table I. Note that unit 3 is an expensive generator. The maximum reserves $R_i^{\mathrm{U,max}}$ and $R_i^{\mathrm{D,max}}$ are assumed to be equal to $P_i^{\max}$ for all units. These units can be therefore scheduled for both energy and reserve. The load L_3, located at node 3, is 230 MW and 320 MW at periods 1 and 2, respectively. A value of lost load equal to \$2000/MWh is considered at the operation stage.

The wind unit is located at node 2. A small production cost of \$0.3/MWh is assumed for this unit. We consider two scenarios, *high* and *low*, to characterize wind production in the intra-day market, and for each second-stage scenario, three scenarios, namely, *high*, *medium* and *low*, are considered at the operation stage. There are in total six scenarios at each time period, as presented in Table II. Also, we assume that these are equi-probable scenarios. The other assumption is that at the first stage, the wind dispatch is within $\pm 20\%$ of its best available forecast $W_{\mathrm{qt}}^{\mathrm{s_1}}$, which are 58 MW and 87 MW at periods 1 and 2, respectively ($\alpha^{\mathrm{WUs_1}} = 1.2$, $\alpha^{\mathrm{WDs_1}} = 0.8$). On the other hand,

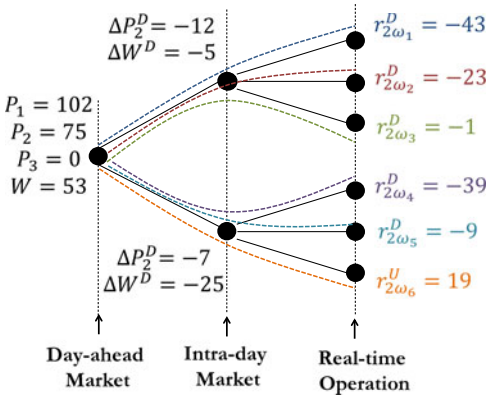

Fig. 3. Dispach, adjustment, and deployed reserves in period 1.

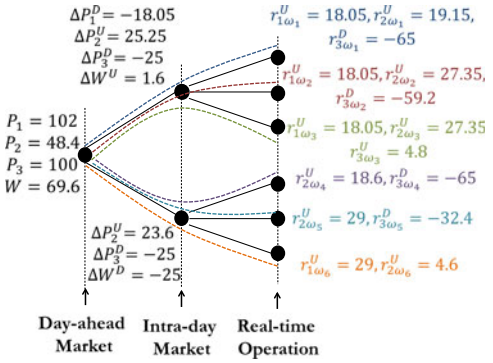

Fig. 4. Dispach, adjustment, and deployed reserves in period 2.

TABLE III
DAY-AHEAD, ADJUSTMENT, AND BALANCING CLEARING PRICES [$/MWH]

		$\lambda^{s2}_{n\omega}/\pi_\omega$		$\lambda^{s3}_{n\omega}/\pi_\omega$		
	λ_n	High	Low	High	Medium	Low
period 1	4.01	4.01	4.01	4.01	4.01	4.01
period 2	4.73	4.73	4.73	4.01	5.09	5.09

the intra-day up and down adjustments of conventional units and wind production are assumed to be limited to 25% of the maximum power outputs and wind installed capacity, respectively ($\alpha_{\Delta P} = \alpha_{\Delta W} = 25\%$).

The results are discussed below. Figs. 3 and 4 show the scheduled quantities, the adjustments, and the deployed reserves for periods 1 and 2, respectively, at the day-ahead market, intra-day market, and the operation stage. Table III provides the day-ahead, adjustment, and balancing clearing prices (the latter two are probability adjusted), denoted by λ_{nt}, $\lambda^{\mathrm{s2}}_{\mathrm{nt}\omega}$, and $\lambda^{\mathrm{s3}}_{\mathrm{nt}\omega}$, respectively. Note that there is no congestion in any of the scenarios considered, hence, prices do not change across nodes. These prices are obtained by fixing the binary variables to their optimal values and solving the resulting LP problem. The dual variables of the energy balance equations of this LP problem are the clearing prices.

Given these schedules and prices, Table IV provides the day-ahead profit (i.e., $\sum_t [P_{\mathrm{it}}(\lambda_{\mathrm{nt}} - C_i) - C^{\mathrm{SU}}_{\mathrm{it}}]$) and the expected profit (i.e., $\sum_t [P_{\mathrm{it}}(\lambda_{\mathrm{nt}} - C_i) - C^{\mathrm{SU}}_{\mathrm{it}} + \sum_\omega \pi_\omega [(\Delta P^{\mathrm{U}}_{\mathrm{it}\omega} - \Delta P^{\mathrm{D}}_{\mathrm{it}\omega})(\lambda^{\mathrm{s2}}_{\mathrm{nt}\omega}/\pi_\omega - C_i) + (r^{\mathrm{U}}_{\mathrm{it}\omega} - r^{\mathrm{D}}_{\mathrm{it}\omega})(\lambda^{\mathrm{s3}}_{\mathrm{nt}\omega}/\pi_\omega - C_i)]]$).

TABLE IV
DAY-AHED AND EXPECTED PROFIT [$]

	unit 1	unit 2	unit 3	wind	Total
DA profit	263.40	24.60	−86.06	504.90	706.90
Total expected profit	263.40	62.50	−53.70	397.50	669.70

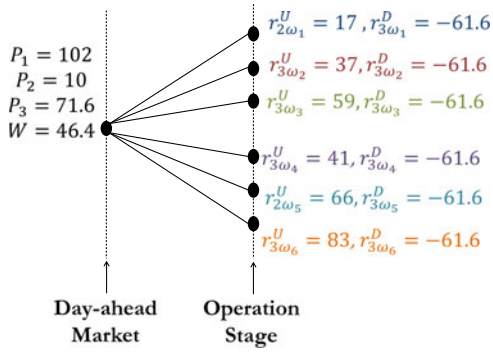

Fig. 5. Production schedules result from two-stage model in period 1.

Focusing on the day-ahead market, unit 3 is not scheduled at period 1, at period 2 it earns $4.73 \times 100 = \$473$, while its total start-up and production cost is $5.09 \times 100 + 50.06 = \$559.06$. Therefore, unit 3 incurs a loss of \$86.06 at the day-ahead market. At the intra-day stage, the profit of unit 3 increases by $(4.73 - 5.09) \times -25 = \$9$ if any of the scenarios *high* or *low* realizes. At the operation stage, the profit of unit 3 increases only under scenarios ω_1 and ω_4. However, none of these increases in profit can cover the loss of \$86.06 at day-ahead market. Therefore, unit 3 suffers a loss on average as well as under any scenario.

In order to avoid this loss, an uplift of \$86.06 is paid to unit 3 and allocated to the load. Note that an uplift is a side-payment given only to those units incurring losses at the day-ahead market. Therefore, the uplift makes losses of these units zero without extra profit and it is calculated based on day-ahead losses of unit i as $\max\{0, \sum_t (P_{\mathrm{it}}(C_i - \lambda_{\mathrm{nt}}) + C^{\mathrm{SU}}_{\mathrm{it}})\}$.

The total expected cost is \$1515.1. Without uplift, the payment of load L_3 at the day-ahead market is $4.01 \times 230 = \$922.3$ and $4.73 \times 320 = \$1513.6$ at periods 1 and 2, respectively. The total payment over the two periods (\$2435.9) is equal to the summation of total profit of producers (\$706.89) and the cost of all units (\$1729) at this stage. Considering the uplift of \$86.06, L_3 finally pays \$2521.95.

A. *Performance of the Three-Stage Model vs. the Two-Stage One*

We present below the outcomes of a two-stage model and compare them to the results from the three-stage model. The scenarios representing the operation stage for the two-stage model are the same as those modeling the operation stage of the three-stage model (RT stage in Table II).

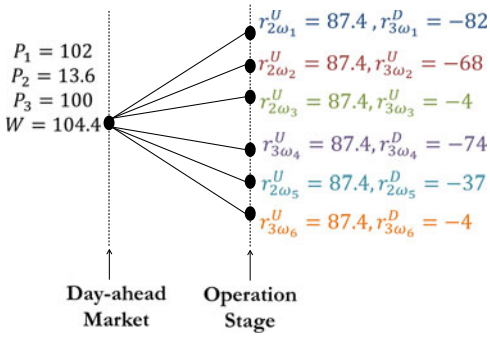

Fig. 6. Production schedules result from two-stage model in period 2.

TABLE V
CLEARING PRICES OBTAINED FROM TWO-STAGE MODEL [$/MWH]

	λ_n	$\lambda_{n\omega_1}$	$\lambda_{n\omega_2}$	$\lambda_{n\omega_3}$	$\lambda_{n\omega_4}$	$\lambda_{n\omega_5}$	$\lambda_{n\omega_6}$
period 1	4.01	4.01	4.01	4.01	4.01	4.01	4.01
period 2	5.09	5.09	5.09	5.09	5.09	5.09	5.09

TABLE VI
COSTS [$]; THREE-STAGE MODEL VS. TWO-STAGE MODEL

	Three-stage model	Two-stage model
Day-ahead market	1729.00	1540.80
Intra-day market	−102.80	–
Operation stage	−111.10	162.70
Total expected cost	1515.10	1703.50

The production schedules for the two-stage model are shown in Figs. 5 and 6 for periods 1 and 2, respectively.

Table V provides the energy and balancing clearing prices obtained from the two-stage model. The day-ahead price at period 2 obtained from the two-stage model are higher than those of the three-stage model. Depending on scenarios, the balancing prices of the two-stage model are equal to or higher than those obtained from the three-stage model. This is the result of the reduced wind scenario information in the two-stage model.

The day-ahead cost (i.e., $\sum_{t=1}^{N_T}[\sum_{i=1}^{N_G}[C^{\mathrm{SU}}_{\mathrm{it}}+C_iP_{\mathrm{it}}]+\sum_{q=1}^{N_Q}C_qW_{\mathrm{qt}}]$), the intra-day cost (i.e., $\sum_{t=1}^{N_T}\sum_{\omega=1}^{N_\Omega}\pi_\omega[\sum_{i=1}^{N_G}(\Delta P^{\mathrm{U}}_{\mathrm{it}\omega}-\Delta P^{\mathrm{D}}_{\mathrm{it}\omega})+\sum_{q=1}^{N_Q}(\Delta W^{\mathrm{U}}_{\mathrm{qt}\omega}-\Delta W^{\mathrm{D}}_{\mathrm{qt}\omega})]$), and the operation cost (i.e., $\sum_{t=1}^{N_T}\sum_{\omega=1}^{N_\Omega}\pi_\omega[\sum_{i=1}^{N_G}(r^{\mathrm{U}}_{\mathrm{it}\omega}-r^{\mathrm{D}}_{\mathrm{it}\omega})+\sum_{q=1}^{N_Q}C_q(W^{s_3}_{\mathrm{qt}\omega}-W_q-\Delta W^{\mathrm{U}}_{\mathrm{qt}\omega}+\Delta W^{\mathrm{D}}_{\mathrm{qt}\omega}-w^{\mathrm{spill}}_{\mathrm{qt}\omega})+\sum_{j=1}^{N_L}V^{\mathrm{LOL}}_{\mathrm{jt}}L^{\mathrm{shed}}_{\mathrm{jt}\omega}]$) for both models are provided in Table VI. The three-stage model results in a higher day-ahead cost than that of the two-stage model, but a lower balancing cost, which finally results in a lower total expected cost. The main reason to have a lower day-ahead cost in the two-stage model is the wind schedules. Wind schedules are directly related to wind information availability. The total wind power scheduled is 150.8 MW over the two periods for the two-stage model, which is higher than the 122.6 MW scheduled for wind production in the three-stage model.

TABLE VII
PRODUCERS PROFIT[$]; THREE-STAGE MODEL VS. TWO-STAGE MODEL AND NO UPLIFT

Three-stage model	unit 1	unit 2	unit 3	wind	all units
Day-ahead	263.40	24.60	−86.00	504.90	706.90
Intra-day	−15.30	17.60	9.00	−107.50	−96.20
Operation	15.30	20.30	23.40	0.00	59.00
Total exp. profit	263.40	62.50	−53.70	397.50	**669.70**
Two-stage model	**unit 1**	**unit 2**	**unit 3**	**wind**	**all units**
Day-ahead	300.07	98.88	−60.86	672.20	1010.30
Operation	0.00	0.00	0.00	0.00	0.00
Total exp. profit	300.07	98.88	−60.86	672.20	**1010.30**

TABLE VIII
CHARACTERISTICS OF THE GENERATING UNITS

Type	U_{90}	U_{50}	U_{155}	U_{76}	U_{197}	U_{400}
Unit i	1	2,4,8	3,6	5	7	9
Node	2	7,15,22	10,18	16	21	23
$P_i^{\max}$ (MW)	90.00	50.00	155.00	76.00	197.00	400.00
$P_i^{\min}$ (MW)	25.00	15.00	55.00	15.20	69.00	100.00
C_i^{SU} ($)	300.00	100.00	320.00	400.00	300.00	1000.00
C_i ($/MW)	19.67	0.00	10.68	11.89	11.09	5.53

Table VII provides the profit of the units (conventional units and wind unit) at each stage and in total for both models without uplift. The total expected profit of producers is lower in the three-stage model than that of two-stage model. This observation does not reverse after adding the uplift, that is $60.86 for the two-stage model and $80.06 for the three-stage model. Note that the unit profits at the operation stage are zero under the two-stage model; the reason is that unit 2 and unit 3 are deployed under balancing prices equal to their marginal costs.

The consumer payment is the summation of cost and profit at the first stage. Given the day-ahead costs and total producer profits, the consumer payment without uplift is $2551.1 for the two-stage model and $2435.9 for the three-stage model. That is, the consumer payment from the two-stage model is higher than that of the three-stage model. Uplift does not change this result, as it increases the consumer payment to $2611.9 and $2521.9 for the two-stage model and the three stage model, respectively.

IV. SIMULATION RESULTS: RTS SYSTEM

This section compares results obtained from the three-stage and two-stage models using a 24-node system based on the single-area IEEE Reliability Test System (RTS) [18]. To facilitate the analysis of the results, we have modified some of the original characteristics of this test system. We consider the system having 34 lines, 9 conventional generating units, and 1 wind power unit. The data of conventional generating units are provided in Table VIII. We assume that hydro units 2,4, and 8 (i.e., U_{50}) offer its energy production at zero price.

Table IX provides the total demand over the 24 periods, while the demand locations and the corresponding shares are as in [19]. The wind power unit is located at node 7. Wind speed data are obtained from the System Advisor Model (SAM) [20].

TABLE IX
TOTAL DEMAND IN [MW] FROM PERIOD 1 TO PERIOD 24

period	1	2	3	4
demand	828.10	831.00	842.00	923.00
period	5	6	7	8
demand	943.00	1103.60	1185.30	1139.00
period	9	10	11	12
demand	1137.50	1121.00	1123.00	1099.00
period	13	14	15	16
demand	1088.00	1100.00	1103.00	1119.00
period	17	18	19	20
demand	1125.00	1143.00	1115.00	1109.00
period	21	22	23	24
demand	1101.20	1080.10	1037.00	800.00

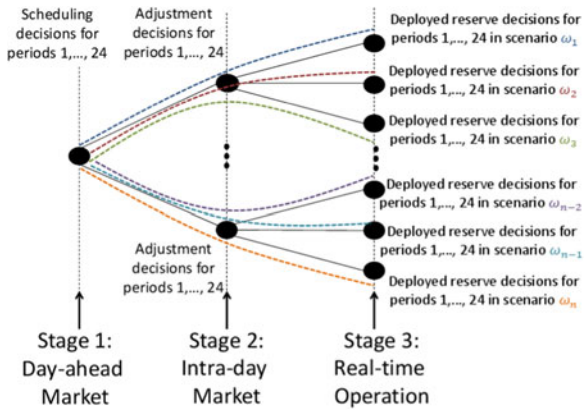

Fig. 7. Scenario tree for the three stages of day-ahead market, intra-day market, and real-time operation. Each scenario involves 24 values for the wind power output of wind unit.

Specifically, we use wind speed data from Austin, Texas, and apply the power curve of a 2-MW wind turbine (Vestas V80/2000 with a hub height of 80 m) to generate the hourly wind-power productions for 24 time periods. The power curve of this turbine model can be found in [21]. The installed capacity is 600 MW.

The following process is used for scenario generation. We generate N_{Ω_1} scenarios (each scenario involves 24 values for the output of the wind power unit pertaining to the 24 time periods of day d) prior to the day-ahead gate closure, using all the historical data available up to this time and an appropriate time-series model. Then, conditioned to the actual values of each scenario during the hours between the day-ahead gate closure and the intra-day gate closure, and using an appropriate time-series model, we generate N_{Ω_2} new scenarios for each one of the original N_{Ω_1} scenarios, resulting in a total number of N_Ω scenarios, where $N_\Omega = N_{\Omega_1} \times N_{\Omega_2}$.

The decision-making tree including scenarios and time periods is shown in Fig. 7.

We consider 10 scenarios at the intra-day market, and corresponding to each second-stage scenario 15 scenarios at the operation stage; therefore, there are in total 150 equi-probable scenarios at each time period for the three-stage model. The corresponding two-stage model is assumed to have the same 150 equi-probable scenarios at the operation stage.

TABLE X
DIMENSION OF THE THREE-STAGE AND TWO-STAGE MODELS

	3-stage Model	2-stage Model
No. of binary variables	216	216
No. of continuous variables	375432	217232
No. of total variables	375648	217248
No. of constraints	786744	409320
Computation time (s)	123	48

TABLE XI
RTS CASE: CURRENT CASE

	3-stage Model		2-stage Model	
Unit i	DA Profit ($)	Exp. Profit ($)	DA Profit ($)	Exp. Profit ($)
1	−8489.42	−4581.29	−10998.97	−3696.75
2	13471.36	13818.44	4575.19	14043.00
3	2175.66	3174.24	3622.79	3896.70
4	13042.15	13400.31	6332.85	14043.00
5	−612.19	282.04	−34.44	136.41
6	2109.44	3269.33	3664.89	3896.70
7	2064.74	2173.20	3435.12	3540.08
8	12954.63	13531.14	4142.90	14043.00
9	42299.73	51345.17	55651.98	59056.00
Wind	16627.21	21358.15	11626.71	11626.71
Total	95643.31	117770.74	82019.03	120584.85
	DA Cost ($)	Exp. Cost ($)	DA Cost ($)	Exp. Cost ($)
	192507.85	174401.51	217498.08	190554.00
	Cons. pay. ($)	Uplift ($)	Cons. pay. ($)	Uplift ($)
	288151.16	9101.61	299517.11	11033.41

For the simulation, we use CPLEX 12.5.0 under MATLAB on a computer with two Intel(R) Core(TM) processors clocking at 2.7 GHz and 8 GB of RAM. The sizes of the proposed models in terms of numbers of variables and constraints, and computation time are provided in Table X. Note that the computation times reported are an indication of the tractability of a three-stage model, and that using industry-grade computers and parallelization should allow achieving appropriate solution times.

The results are presented below following this order: we first present the outcomes of a base case study involving a single load profile. Next, we consider different bounds for the system constraints using the same load profile and explore how these bounds influence the results. Finally, different load profiles and different bounds are considered.

A. Base Case

This case study maintains the assumptions used in the illustrative example, namely $\alpha^{\mathrm{WUs}_1} = \alpha^{\mathrm{WUs}_2} = 1.2$, $\alpha^{\mathrm{WDs}_1} = \alpha^{\mathrm{WDs}_2} = .8$, $\alpha_{\Delta W} = 0.25\%$, $\alpha_{\Delta P} = 0.25\%$, and the limit of reserve capacity is equal to the production capacity of each conventional unit.

Table XI provides details regarding day-ahead profit, expected profit, day-ahead cost, expected cost, and consumer payment resulting from both models without uplift. Under both models, U_{90} and U_{76} incur losses at the day-ahead market, but

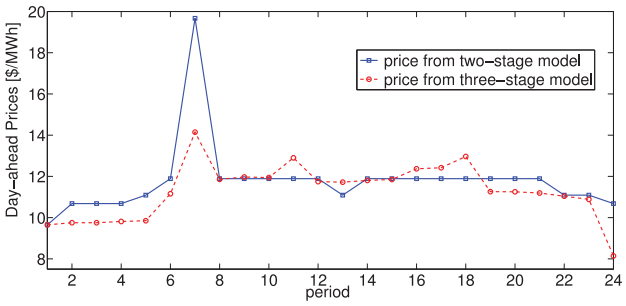

Fig. 8. Day-ahead clearig prices from the three-stage model (blue) and the two-stage model (red) over all periods.

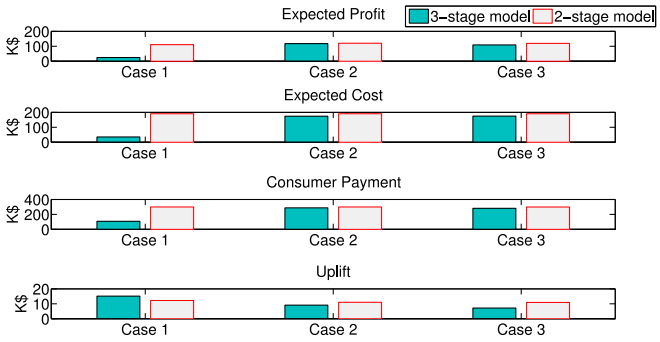

Fig. 9. Expected profit, expected cost, consumer payment, and uplift for different cases.

only U_{90} has a negative expected profit. The total producer profit at the market stage is higher in the three-stage model than in the two-stage model, whereas the total expected profit from the three-stage model is lower than that of the two-stage model. The main reason is that power scheduled from the wind unit is higher under the three-stage model than under the two-stage model. This is the result of information asymmetry on wind production. Also, the three-stage model results in lower day-ahead cost, expected cost, and consumer payment than those from the two-stage model. The savings in expected cost and consumer payment obtained in the three-stage model as a percentage of the corresponding values in the two-stage model are 8.48% and 3.79%, respectively.

For the purpose of comparing day-ahead prices, Fig. 8 shows the day-ahead prices obtained from the three-stage and two-stage models. At period 7 (morning peak), the two-stage model results in a higher price than that of the three-stage model. Also, at period 24 (when the lowest load occurs) the price from the three-stage model is considerably lower than that of the two-stage model. Despite the higher prices obtained from the two-stage model over several periods, an uplift of $11,033.41 is still required and it is higher than the uplift of the three-stage model ($9101.00).

B. Analyses of Flexibility of Units for Reserve Provision and Different Adjustment Bounds

To investigate the impact of availability of reserves and limits on the intra-day adjustments, we consider the following cases:

1) *Case 1 (not limited):*
   a) All conventional units provide reserves: $R_i^{\mathrm{U,max}} = R_i^{\mathrm{D,max}} = P_i^{\max}, \forall i$.
   b) Wind production at the day-ahead market is limited by the wind installed capacity. That is, the limit of the wind unit is $0 \le W_{\mathrm{qt}} \le W_q^{\max}$ in the day-ahead market (constraint (1d)). Also, for consistency, $0 \le W_{\mathrm{qt}} + \Delta W_{\mathrm{qt}\omega}^{\mathrm{U}} - \Delta W_{\mathrm{qt}\omega}^{\mathrm{D}} \le W_q^{\max}$ (constraint (1k)).
   c) The up/down wind adjustments are limited by the wind installed capacity at the intra-day market. That is, $\Delta W_{\mathrm{qt}\omega}^{\mathrm{U}} \le W_q^{\max}$ and $\Delta W_{\mathrm{qt}\omega}^{\mathrm{D}} \le W_q^{\max}$ (i.e., $\alpha_{\Delta W} = 1$ in constraint (1 m)).
   d) Up/down adjustments of conventional units are up to their maximum power output. That is, $\alpha_{\Delta P} = 1$ in constraint (1l), and thus, $\Delta P_{\mathrm{it}\omega}^{\mathrm{U}} \le P_i^{\max}$ and $\Delta P_{\mathrm{it}\omega}^{\mathrm{D}} \le P_i^{\max}$.
2) *Case 2 (partly limited):*
   a) All conventional units provide reserves: $R_i^{\mathrm{U,max}} = R_i^{\mathrm{D,max}} = P_i^{\max}, \forall i$.
   b) Wind production at the day-ahead market is limited at $\pm 20\%$ of the best available wind production forecast. That is, $\alpha^{\mathrm{WDs_1}} = 0.8$ and $\alpha^{\mathrm{WUs_1}} = 1.2$, and thus, $0.8W_{\mathrm{qt}}^{\mathrm{s_1}} \le W_{\mathrm{qt}} \le 1.2W_{\mathrm{qt}}^{\mathrm{s_1}}$ (constraint (1d)).
   c) The up/down production and wind adjustments at the intra-day stage are limited by 25% of installed capacity. That is, $\alpha_{\Delta P} = \alpha_{\Delta W} = 0.25$, and thus, $\Delta P_{\mathrm{it}\omega}^{\mathrm{U}} \le 0.25P_i^{\max}$ and $\Delta P_{\mathrm{it}\omega}^{\mathrm{D}} \le 0.25P_i^{\max}$, and $\Delta W_{\mathrm{qt}\omega}^{\mathrm{U}} \le 0.25W_q^{\max}$ and $\Delta W_{\mathrm{qt}\omega}^{\mathrm{D}} \le 0.25W_q^{\max}$.
3) *Case 3 (fully limited):*
   a) Nuclear and hydro units (U_{400} and U_{50}) do not provide reserves.
   b) Wind production at the day-ahead market is limited at $\pm 20\%$ of the best available wind production forecast. That is, $\alpha^{\mathrm{WDs_1}} = 0.8$ and $\alpha^{\mathrm{WUs_1}} = 1.2$, and thus, $0.8W_{\mathrm{qt}}^{\mathrm{s_1}} \le W_{\mathrm{qt}} \le 1.2W_{\mathrm{qt}}^{\mathrm{s_1}}$ (constraint (1d)).
   c) The up/down production and wind adjustments at the intra-day stage are limited by 25% of installed capacity. That is, $\alpha_{\Delta P} = \alpha_{\Delta W} = 0.25$, and thus, $\Delta P_{\mathrm{it}\omega}^{\mathrm{U}} \le 0.25P_i^{\max}$ and $\Delta P_{\mathrm{it}\omega}^{\mathrm{D}} \le 0.25P_i^{\max}$, and $\Delta W_{\mathrm{qt}\omega}^{\mathrm{U}} \le 0.25W_q^{\max}$ and $\Delta W_{\mathrm{qt}\omega}^{\mathrm{D}} \le 0.25W_q^{\max}$.

TABLE XII
SAVINGS IN THE EXPECTED COSTS AND CONSUMER PAYMENT FOR THE DIFFERENT CASE STUDIES

	Saving in expected cost (%)	Saving in consumer payment (%)
Case 1	81.54	63.91
Case 2	8.48	3.79
Case 3	8.19	5.61

Fig. 9 shows that the total expected profit, the expected cost, and the consumer payment obtained from the two-stage model are higher than those of the three-stage model. The savings in expected cost and consumer payment obtained in the three-stage model as a percentage of the corresponding values in the two-stage model are provided in Table XII. The difference

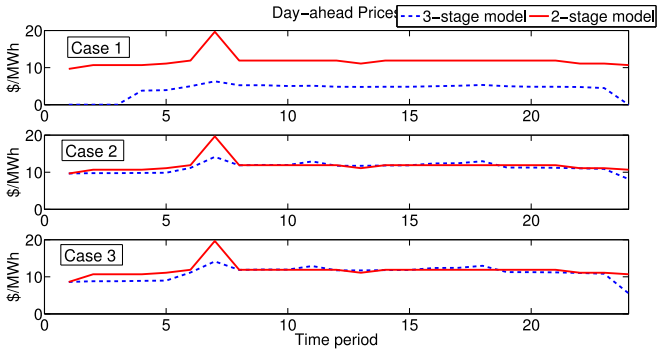

Fig. 10. Day-ahead clearing prices for different cases.

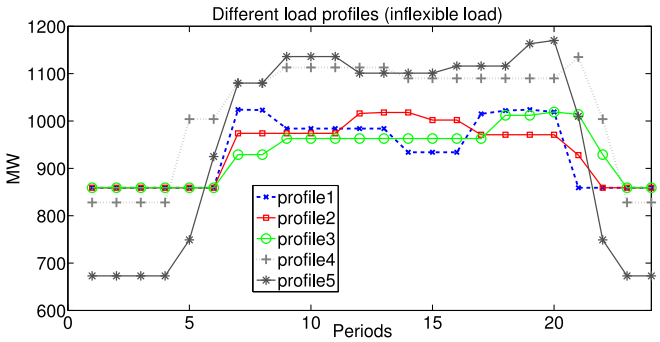

Fig. 11. Different load profiles.

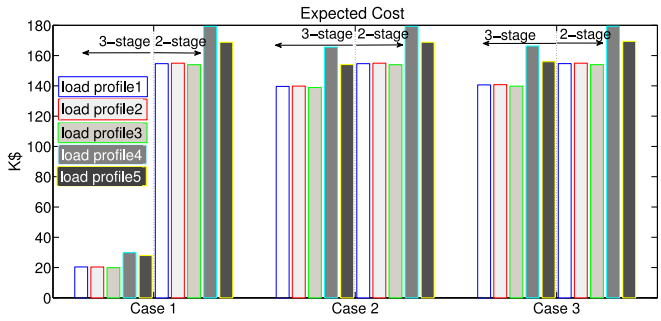

Fig. 12. Expected costs for different load profiles and different limited cases.

TABLE XIII
SAVINGS IN EXPECTED COST AND CONSUMER PAYMENT FOR THE DIFFERENT LOAD PROFILES [%]

	Savings of exp. cost			Savings of CP		
Load profile	case 1	case 2	case 3	case 1	case 2	case 3
1	86.80	9.72	9.07	75.78	6.29	11.85
2	86.85	9.75	9.16	74.60	6.34	11.94
3	87.07	9.79	9.20	73.75	6.71	12.63
4	83.36	7.66	7.28	66.22	3.18	5.42
5	83.42	8.71	7.93	67.44	7.57	8.75

between these outcomes is large for case 1 (less restricted), and small for case 2 and case 3 for more restricted cases. Therefore, irrespective of the limits imposed on reserves and intra-day unit adjustments, we conclude that the three-stage model has a better performance from the consumer point of view. The uplift, however, follows a different trend (bottom plot in Fig. 9). The three-stage model results in a larger uplift for case 1, while a smaller uplift for case 2 and case 3 than those of the two-stage model. The uplift from the two-stage model is similar in all cases; however the uplift from the three-stage model decreases along with the increase in the restrictions. Note that the uplift amount is small and does not reverse the fact that the consumer payment of the three-stage model is smaller. Understanding this is easy by observing the day-ahead prices in Fig. 10. The prices from the three-stage model are lower in case 1 than those in cases 2 and 3. This results in smaller uplifts in cases 2 and 3. Also, these prices are in the same order of magnitude as the day-ahead prices from the two-stage model, and hence, the consumer payments are in the same order of magnitude in case 2 and case 3. In addition, the day-ahead prices from the three-stage model and those from the two-stage model get closer to each other as cases become increasingly restricted.

We also simulate these models on different load profiles (shown in Fig. 11) and observe similar outcomes. Fig. 12 shows that a higher expected cost is obtained by using the two-stage model than that of the three-stage model irrespective of the limiting bounds for five different load profiles and the different cases. Note that the large difference between expected costs of the three stage model and the two stage model for case 1 is due to the wide (and rather unrealistic) bounds assumed for the intra-day adjustments of the wind unit as well as conventional units. The expected costs of the three-stage model get closer to those from the two-stage model when limiting these bounds, as in case 2 and case 3.

Table XIII provides the savings in expected cost and consumer payment obtained in the three-stage model as a percentage of the corresponding values in the second-stage model. The savings in case 1 are large due to the wide (unrealistic) bounds assumed for the intra-day adjustments of the wind unit as well as the conventional units.

The standard deviations for the different load profiles considered and the different cases analyzed are provided in Table XIV below. The standard deviations of both models are of the same order of magnitude for case 1 (all load profiles). For case 2, the standard deviations from the two-stage model are smaller than those from the three-stage model. This observation is, however, reversed for case 3. Therefore, a general conclusion regarding the standard deviation of cost from these instances cannot be obtained. In other words, none of these models guarantee a smaller variability of cost as compared to the other one. Note that the three-stage model improves the cost in term of expectation, but the variability of the cost around the expected value is similar to that of the two-stage model.

To show the benefits of the proposed three-stage model, we compare the value of stochastic solution (VSS) [22] for both the three-stage and two-stage models. The value of stochastic solution is computed as follows. The uncertain wind power output is replaced by its mean value, and a deterministic problem without recourse is solved. We call the solution of this problem corre-

TABLE XIV
STANDARD DEVIATIONS FROM THE THREE-STAGE MODEL AND THE TWO-STAGE MODEL FOR THE DIFFERENT LOAD PROFILES [$]

	Case 1		Case 2		Case 3	
Load profile	3-stage model	2-stage model	3-stage model	2-stage model	3-stage model	2-stage model
1	1.10e+04	3.61e+04	3.08e+04	7.45e+03	7.58e+03	1.32e+04
2	1.05e+04	3.53e+04	3.04e+04	6.71e+03	9.20e+03	1.18e+04
3	9.30e+03	4.33e+04	2.95e+04	7.84e+03	6.28e+03	1.21e+04
4	1.09e+04	4.52e+04	3.57e+04	6.76e+03	1.02e+04	1.34e+04
5	1.19e+04	4.04e+04	3.28e+04	1.44e+04	7.34e+03	8.74e+03

TABLE XV
THE VSS [%]

	Three-stage model			Two-stage model		
Load profile	case 1	case 2	case 3	case 1	case 2	case 3
1	4.94	0.32	0.31	0.01	0.01	0.01
2	4.96	0.12	0.11	0.01	0.01	0.01
3	5.06	0.23	0.22	0.01	0.01	0.01
4	3.79	1.31	1.30	6.19	6.19	6.19
5	3.71	0.22	0.22	1.41	1.41	1.41

TABLE XVI
COMPUTATION TIME FOR DIFFERENT NUMBER OF SCENARIOS IN THE SECOND STAGE (10 UNITS, 24 BUSES, 15 SCENARIOS IN THE THIRD STAGE)

No. of scenarios in the second stage	10	15	20
No. of scenarios in the third stage	15	15	15
Total No. of scenarios	150	225	300
Total No. of constraints	786,744	1,179,264	1,571,784
Total No. of decision variables	375,648	562,848	750,048
Expected cost ($)	1.74e+05	1.77e+05	1.77e+05
Computation time (s)	123	235	445

TABLE XVII
COMPUTATION TIME FOR DIFFERENT NUMBER OF SCENARIOS IN THE THIRD STAGE (10 UNITS, 24 BUSES, 10 SCENARIOS IN THE SECOND STAGE)

No. of scenarios in the second stage	10	10	10
No. of scenarios in the third stage	15	25	35
Total No. of scenarios	150	250	350
Total No. of constraints	786,744	1,317,144	1,847,544
Total No. of decision variables	375,648	562,848	750,048
Expected cost ($)	1.74e+05	1.77e+05	1.77e+05
Computation time (s)	123	147	491

sponding to first-stage variables x^{MV}. Next, the first-stage variables in the stochastic problem are fixed at the solution x^{MV}, and the problem is solved. Denoting the optimal objective-function value of this problem z^{D}, the VSS is $\frac{z^{D}-z^{*}}{z^{*}}$, where z^{*} is the optimal objective-function value of the stochastic problem. We note that VSS is not uniquely defined in multi-stage problems [23]. However, the above definition makes the VSS consistent for the three-stage and the two-stage models.

The results are provided in Table XV. The three-stage model has a better performance than the two-stage model (i.e, higher VSS) for all case studies except for those pertaining to load profile 4. In this case, the use of x^{MV} causes load-shedding in real time after the wind power is realized. This results in a high cost, and consequently, a large difference between the optimal value of the two-stage model and that of the deterministic model.

C. Computation Time

In this section, we elaborate on the computational aspect of the proposed model by considering different number of scenarios and different number of units, as follow.

First, we fix the number of scenarios to 15 in the third stage and consider different numbers of scenarios in the second stage. The corresponding computation time and the expected cost are provided in Table XVI.

The computation time increases with the problem size. However, it remains within an acceptable range (e.g., less than 8 minute for a problem size larger than 0.7 million variables and 1.5 million constraints). The increases in the total number of scenarios (from 150 to 225 and from 150 to 300) result in the same expected cost, which is slightly higher than the expected cost obtained in the case with 150 scenarios. In other words, the sensitivity of the expected cost decreases as the number of second-stage scenarios increases.

Table XVII provides the computation time for different number of the scenarios in the third stage if the number of the second-stage scenarios is fixed to 10. The computation time does not change significantly from 150 scenarios to 250 scenarios, while it increases to 491 s if considering 350 scenarios, for which the size of the problem is significantly larger (i.e., 1.8 million of constraints and 0.9 million of variables). The increases in the total number of scenarios (from 150 to 250 and from 150 to 350) result in the same expected cost, which is slightly higher than the expected cost obtained in the case with 150 scenarios. In other words, the sensitivity of the expected cost decreases as the number of third-stage scenarios increases.

Given Tables XVII and XVI, we infer that the sensitivity of the expected cost decreases as the total number of scenarios increases.

In short, an increase in the number of scenarios involves a better uncertainty description, and hence, a possible change in expected cost. However, this is valid up to a certain number of scenarios (in the case study, 225). Once this number of scenarios is reached, the uncertainty description is accurate enough and

TABLE XVIII
COMPUTATION TIME FOR THE DIFFERENT NUMBER OF GENERATORS (24 BUSES, 150 SCENARIOS)

No. of units	10	15	20
No. of binary variables	216	336	456
Total No. of decision variables	375,648	448,008	520,368
Total No. of constraints	786,744	964,944	1,143,144
Expected cost ($)	1.74e+05	1.75e+05	1.75e+05
Computation time (s)	123	182	590

the expected cost remains unaltered. If this number of scenarios is increased, the expected cost remains the same, whereas computation time increases.

Finally, Table XVIII provides computation times for different number of units if 150 scenarios are considered. With the increase in the number of units, the size of the problem and the number of binary commitment variables increase, and hence, the computation time increases as well that is not beneficial.

We note that incorporating an AC network representation will not change the conclusions of the study, as active and reactive powers are fairly decoupled in transmission networks. However, a possible way to incorporate an AC network representation in our analysis is through convex relaxation techniques [24]. Nevertheless, the use of such techniques is outside the scope of this paper.

V. CONCLUSION

We present a three-stage stochastic model to clear the day-ahead market, which explicitly represents an intra-day market and the real-time operation. We then compare the outcomes of this model with results from a two-stage model, which includes a prognosis solely of real-time operation.

The simulation outcomes show that the proposed three-stage model has a better performance than the two-stage one as a result of more informed decisions at the day-ahead market. These outcomes clearly suggest that replacing a deterministic model with a three-stage model, not a two-stage one, has clear advantages. In other words, if the industry decides to move toward using a a stochastic clearing algorithm (and if it has sufficient computational resources to do so), such a clearing algorithm should be a three-stage one, not a two-stage one.

ACKNOWLEDGMENT

Disclaimer: The views expressed in this paper are solely those of the authors and do not necessarily represent those of Swissgrid.

REFERENCES

[1] A. J. Conejo, M. Carrion, and J. M. Morales. *Decision Making Under Uncertainty in Electricity Markets*. New York, NY, USA: Springer, 2010.
[2] F. Bouffard, F. D. Galiana, and A. J. Conejo, "Market-clearing with stochastic security-part I: Formulation," *IEEE Trans. Power Syst.*, vol. 20, no. 4, pp. 1818–1826, Nov. 2005.
[3] F. Bouffard and F. D. Galiana, "Stochastic security for operations planning with significant wind power generation," in *Proc. 2008 IEEE Power Energy Soc. General Meeting - Convers. Del. Elect. Energy 21st Century*, Jul. 2008, pp. 1–11.
[4] P. A. Ruiz, C. R. Philbrick, E. Zak, K. W. Cheung, and P. W. Sauer, "Uncertainty management in the unit commitment problem," *IEEE Trans. Power Syst.*, vol. 24, no. 2, pp. 642–651, May 2009.
[5] J. M. Morales, A. J. Conejo, and J. Perez-Ruiz, "Economic valuation of reserves in power systems with high penetration of wind power," *IEEE Trans. Power Syst.*, vol. 24, no. 2, pp. 900–910, May 2009.
[6] A. Papavasiliou, S. S. Oren, and R. P. O'Neill, "Reserve requirements for wind power integration: A scenario-based stochastic programming framework," *IEEE Trans. Power Syst.*, vol. 26, no. 4, pp. 2197–2206, Nov. 2011.
[7] J. M. Morales, A. J. Conejo, K. Liu, and J. Zhong, "Pricing electricity in pools with wind producers," *IEEE Trans. Power Syst.*, vol. 27, no. 3, pp. 1366–1376, Aug. 2012.
[8] D. Bertsimas, D. Brown, and C. Caramanis, "Theory and applications of robust optimization," *SIAM Rev.*, vol. 53, no. 3, pp. 464–501, 2011.
[9] D. Bertsimas, E. Litvinov, X. A. Sun, J. Zhao, and T. Zheng, "Adaptive robust optimization for the security constrained unit commitment problem," *IEEE Trans. Power Syst.*, vol. 28, no. 1, pp. 52–63, Feb. 2013.
[10] R. Jiang, J. Wang, and Y. Guan, "Robust unit commitment with wind power and pumped storage hydro," *IEEE Trans. Power Syst.*, vol. 27, no. 2, pp. 800–810, May 2012.
[11] M. Zugno and A. J. Conejo, "A robust optimization approach to energy and reserve dispatch in electricity markets," *Eur. J. Oper. Res.*, vol. 247, no. 2, pp. 659–671, 2015.
[12] H. Ye, J. Wang, and Z. Li, "Robust integration of high-level dispatchable renewables in power system operation," Dec. 2015. arXiv:1512.06036.
[13] Y. Dvorkin, H. Pandzic, M. A. Ortega-Vazquez, and D. S. Kirschen, "A hybrid stochastic/interval approach to transmission-constrained unit commitment," *IEEE Trans. Power Syst.*, vol. 30, no. 2, pp. 621–631, Mar. 2015.
[14] Y. Wang, Q. Xia, and C. Kang, "Unit commitment with volatile node injections by using interval optimization," *IEEE Trans. Power Syst.*, vol. 26, no. 3, pp. 1705–1713, Aug. 2011.
[15] C. Zhao and Y. Guan, "Unified stochastic and robust unit commitment," *IEEE Trans. Power Syst.*, vol. 28, no. 3, pp. 3353–3361, Aug. 2013.
[16] P. A. Ruiz, C. R. Philbrick, and P. W. Sauer, "Modeling approaches for computational cost reduction in stochastic unit commitment formulations," *IEEE Trans. Power Syst.*, vol. 25, no. 1, pp. 588–589, Feb. 2010.
[17] F. Bouffard, F. D. Galiana, and A. J. Conejo, "Market-clearing with stochastic security-part II: Case studies," *IEEE Trans. Power Syst.*, vol. 20, no. 4, pp. 1827–1835, Nov. 2005.
[18] P. Wong *et al.*, "The IEEE reliability test system-1996," *IEEE Trans. Power Syst.*, vol. 14, no. 3, pp. 1010–1020, Aug. 1999.
[19] C. Ruiz, A. J. Conejo, and S. A. Gabriel, "Pricing non-convexities in an electricity pool," *IEEE Trans. Power Syst.*, vol. 27, no. 3, pp. 1334–1342, Aug. 2012.
[20] Alliance for Sustainable Energy (Alliance), National Renewable Energy Laboratory, Golden, CO, USA. Solar advisor model version 2012.5.11.
[21] Danish Wind Industry Association. Wind Turbine Power Calculator. [Online]. Available: http://www.windpower.org
[22] J. R. Birge and F. Louveaux, *Introduction to Stochastic Programming* (Springer Series in Operations Research and Financial Engineering). New York, NY, USA: Springer, 2011.
[23] L. F. Escudero, A. Garín, M. Merino, and G. Pérez, "The value of the stochastic solution in multistage problems," *TOP*, vol. 15, no. 1, pp. 48–64, 2007.
[24] R. Madani, S. Sojoudi, and J. Lavaei, "Convex relaxation for optimal power flow problem: Mesh networks," *IEEE Trans. Power Syst.*, vol. 30, no. 1, pp. 199–211, Jan. 2015.

Farzaneh Abbaspourtorbati (S'15) received the M.Sc. degree from ETH Zurich, Zurich, Switzerland, in 2011 and is currently working toward the Ph.D. degree in the power system group, École Polytechnique Fédérale de Lausanne, Lausanne, Switzerland. She is currently with TSO Market Development team at Swiss Transmission System Operator, Swissgrid.

Antonio J. Conejo (F'04) received the M.S. degree from MIT, Cambridge, MA, USA, in 1987, and the Ph.D. degree from the Royal Institute of Technology, Stockholm, Sweden, in 1990. He is currently a Professor at the Integrated System Engineering and the Electrical & Computer Engineering Departments, The Ohio State University, Columbus, OH, USA. His research interests include control, operations, planning, economics, and regulation of electric energy systems, as well as statistics and optimization theory and its applications.

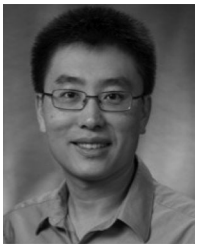

Jianhui Wang (M'07–SM'12) received the Ph.D. degree in electrical engineering from Illinois Institute of Technology, Chicago, IL, USA, in 2007. Currently, he is the Section Lead for Advanced Power Grid Modeling at the Energy Systems Division, Argonne National Laboratory, Argonne, IL, USA. He is also an Affiliate Professor at Auburn University, Auburn, AL, USA and an Adjunct Professor at University of Notre Dame, Notre Dame, IN, USA. He has held visiting positions in Europe, Australia, and Hong Kong including a VELUX Visiting Professorship at the Technical University of Denmark. He is the secretary of the IEEE Power & Energy Society (PES) Power System Operations Committee. He is an Associate Editor of the *Journal of Energy Engineering* and an editorial board member of *Applied Energy*.

Dr. Wang is the Editor-in-Chief of the IEEE TRANSACTIONS ON SMART GRID and an IEEE PES Distinguished Lecturer. He also received the IEEE PES Power System Operation Committee Prize Paper Award in 2015.

Rachid Cherkaoui (SM'07) received the M.S. degree in electrical engineering and the Ph.D. degree from École Polytechnique Fédérale de Lausanne (EPFL), Lausanne, Switzerland, in 1983 and 1992, respectively. From 1992 to 2009, he was leading the research activities in the field of optimization and simulation techniques applied to electrical power and distribution systems. Since 2009, as a Senior Scientist, he is the head of the power system group, EPFL. Currently, the main research topics of his group are concentrated on electricity market deregulation, distributed generation and storage with reference to distribution systems and smart grids, and power system vulnerability mitigation.